Ecosystem carbon dynamics differ between tundra shrub types in the western Canadian Arctic

Environmental Research Letters

LETTER

Ecosystem carbon dynamics differ between tundra shrub types in the western Canadian Arctic

Lorna E Street[1,2,7], **Jens-Arne Subke**[3], **Robert Baxter**[4], **Kerry J Dinsmore**[5], **Christian Knoblauch**[6] and **Philip A Wookey**[1,3]

1 School of Life Sciences, Heriot-Watt University, Edinburgh EH14 4AS, United Kingdom
2 School of GeoSciences, University of Edinburgh, Edinburgh, EH9 3FF, United Kingdom
3 Biological and Environment Sciences, Faculty of Natural Sciences, University of Stirling, FK9 4LA, United Kingdom
4 School of Biological and Biomedical Sciences, University of Durham, Durham DH1 3LE, United Kingdom
5 Centre for Ecology and Hydrology, Bush Estate, Penicuik EH26 0QB, United Kingdom
6 Institute of Soil Science, Universität Hamburg, Allende-Platz 2, 20146 Hamburg, Germany
7 Author to whom any correspondence should be addressed.

E-mail: Lorna.Street@ed.ac.uk

Keywords: allocation, biomass production efficiency, carbon use efficiency, photosynthesis, respiration, ^{13}C labelling, nitrogen

Supplementary material for this article is available online

OPEN ACCESS

RECEIVED
16 April 2018

REVISED
5 July 2018

ACCEPTED FOR PUBLICATION
13 July 2018

PUBLISHED
31 July 2018

Abstract

Shrub expansion at high latitudes has been implicated in driving vegetation 'greening' trends and may partially offset CO_2 emissions from warming soils. However, we do not yet know how Arctic shrub expansion will impact ecosystem carbon (C) cycling and this limits our ability to forecast changes in net C storage and resulting climate feedbacks. Here we quantify the allocation of photosynthate between different ecosystem components for two common deciduous Arctic shrubs, both of which are increasing in abundance in the study region; green alder (*Alnus viridis* (Chaix) DC.) and dwarf birch (*Betula glandulosa* Michx., B.). Using ^{13}C isotopic labelling, we show that carbon use efficiency (i.e. the fraction of gross photosynthesis remaining after subtracting respiration) in peak growing season is similar between the two shrubs (56 ± 12% for *A. viridis*, 59 ± 6% for *B. glandulosa*), but that biomass production efficiency (plant C uptake allocated to biomass production, per unit gross photosynthesis) is 56 ± 14% for *A. viridis*, versus 31 ± 2% for *B. glandulosa*. A significantly greater proportion of recent photosynthate is allocated to woody biomass in *A. viridis* dominated plots (27 ± 5%), compared to plots dominated by *B. glandulosa* (4 ± 1%). Allocation of C to belowground pools also differs significantly; after 2.5 weeks we recovered 28 ± 6% of recent photosynthate in root-free soil under *B. glandulosa*, but under *A. viridis* we were unable to detect recent photosynthate in the soil. We provide the first evidence that the impact of shrub expansion on Arctic C cycling will be species dependant. Where *Betula* dominates, ~1/3 of recently photosynthesised C will be rapidly allocated belowground to soil and microbial pools. Where *Alnus* dominates, more recently fixed C will be allocated to woody biomass. We conclude that models driven by remotely-sensed aboveground canopy characteristics alone (i.e. greenness) will be unable to accurately represent the impact of vegetation change on Arctic C storage.

Introduction

Shrub expansion is occurring in many tundra ecosystems and has been linked to widespread patterns of vegetation 'greening' across the Arctic (Sturm *et al* 2001, Myers-Smith *et al* 2011, Forbes *et al* 2010, Jia *et al* 2009). Greater photosynthetic CO_2 uptake by more productive Arctic vegetation has the potential to compensate for expected carbon (C) losses from warming permafrost soils over the next decades (Schuur *et al* 2015); recent model-based estimates suggest that increased plant growth at high latitudes will offset permafrost emissions until about mid-century (Schaefer *et al* 2011, Koven *et al* 2011). Field-based observations, however, suggest a different pattern, with more highly productive forest and shrub vegetation associated with

less total ecosystem C storage than neighbouring tundra (Hartley *et al* 2012, Parker *et al* 2015, Wilmking *et al* 2006). If these field observations reflect a widespread phenomenon, 'Arctic greening' may not offset permafrost C release to the extent currently predicted, and we risk underestimating future permafrost C cycle-climate feedbacks (Abbot *et al* 2016). The key issue is that enhanced photosynthetic activity in vegetation may also be accompanied by changes in the way C is allocated throughout the plant-soil system, which in turn can modify rates of C turnover, and thus the trajectory of total stocks. Understanding patterns of plant C allocation in tundra shrubs is therefore a prerequisite for understanding the impact of greening on Arctic C cycle-climate feedbacks.

Carbon partitioning in plants is critical in determining ecosystem C sink strength in a number of ways (Bradford and Crowther 2013). Firstly, the proportion of gross photosynthesis (gross primary productivity, GPP) used to produce new organic matter within the plant, versus that immediately re-respired, determines the total input of fixed C to the ecosystem per unit time. This total flux of fixed C is how we define net primary productivity (NPP) here (Roxburgh *et al* 2005), and thus the ratio of NPP:GPP is equivalent to ecosystem carbon-use-efficiency (CUE). Not all NPP is used for plant growth; this term includes C allocated to non-plant biomass pools such as volatile organic compounds (VOCs), root-exudates and root symbionts. In this study we assume that VOC emissions contribute only a small fraction of NPP (VOC fluxes were $<0.01\%$ of gross photosynthesis in Arctic birch forest at a similar latitude (Faubert *et al* 2012). Recent work suggests that CUE across biomes may be tightly-constrained at around 0.5 as a result of the close biochemical interdependence between respiration and photosynthesis, but that plant growth per unit GPP (the biomass-production-efficiency, BPE) varies substantially—largely in response to site fertility (Campioli *et al* 2015, Vicca *et al* 2012). Predicting plant growth from GPP within terrestrial ecosystem models has been identified as a major source of uncertainty in modelling the changing C balance of northern permafrost regions, partly because the difference between BPE and CUE is often ignored (Xia *et al* 2017).

Once C is fixed from the atmosphere, plant C allocation between biomass pools and the expected lifetime of C in those pools (Street *et al* 2013) determines the size of plant C stocks over time. Rates of C turnover can differ by orders of magnitude between plant tissues; the mean residence time (MRT) of C in wood might be decades or centuries, while the MRT of C in leaves or fine roots may only be days or weeks. The greater the amount of carbon, per unit of increasing plant productivity, that is allocated to long-lived biomass pools, the greater the expected long-term carbon sequestration potential of Arctic vegetation (Hobbie *et al* 1998).

The influence of plant C allocation on ecosystem carbon sink strength is not limited to productivity and patterns of biomass allocation. It is now well-established that belowground C allocation to non-plant pools (root exudates and root-associated symbionts) can directly moderate or 'prime' rates of soil organic matter (SOM) turnover in the rhizosphere (the soil immediately surrounding and influenced by roots) and thus impact soil C stocks (Kuzyakov *et al* 2000, Walker *et al* 2016). In Arctic systems, rhizosphere priming effects (RPEs; an increase in the rate of SOM decomposition in the presence of plants compared with the rate of decomposition in plant-free soil) associated with ectomycorrhizal (ECM) fungi have been implicated as an over-riding factor explaining smaller total terrestrial carbon stocks under deciduous shrub and tree vegetation compared to ericaceous heath tundra (Parker *et al* 2015, Hartley *et al* 2012). Plant partitioning of C to non-plant pools belowground, and thus the significance of RPEs, may therefore be critical in determining tundra C balance as shrubs expand.

In many regions, tundra shrub expansion involves patch expansion, infilling and encroachment of tall deciduous shrubs into sedge or ericaceous dwarf shrub-dominated plant communities (Lantz *et al* 2013, Fraser *et al* 2014). Tall deciduous shrub vegetation ($>$ 0.4 m) in the Arctic is dominated by three genera; *Salix*, *Betula* and *Alnus* (Myers-Smith *et al* 2011), all of which share a woody growth form and are able to form ECM associations. *Alnus* species are also able to gain N from specialized root nodules through symbiosis with N-fixing bacteria of the genus *Frankia* (Mitchell and Ruess 2009b, Horton *et al* 2013). At our study site, *Alnus viridis (Chaix) DC.* and *Betula glandulosa Michx.* dominate the tall deciduous shrub vegetation, with *Salix* confined to riparian areas.

In this study we address the question: do ecosystem C dynamics differ between the common deciduous shrub types currently expanding in the NW Canadian Arctic? Specifically: (1) does ecosystem CUE and BPE differ between vegetation dominated by *A. viridis* versus vegetation dominated by *B. glandulosa*? (2) How does the allocation of recent photosynthate to aboveground and belowground biomass, as well as non-plant pools belowground, differ between these shrub types? Our expectation was that CUE would be similar between shrub types, but that BPE would be greater for *Alnus* because N inputs from symbiotic fixation would increase overall plant N availability, and thus reduce the need for non-plant-biomass C allocation (e.g. to ECMs) belowground. This study is the first to quantify and compare patterns of C allocation common deciduous shrub species expanding into the tundra biome and thus provides crucial insight—and data—to support predictions of terrestrial Arctic C balance.

Materials and methods

We use ^{13}C isotopic pulse-chase labelling methods to quantify ecosystem CUE, BPE and C allocation patterns. Vegetation in 0.64 m^2 experimental plots was exposed to isotopically enriched $^{13}CO_2$ for approx. 2 hrs, and the fate of the photosynthesised ^{13}C label was then monitored over a period of 18 days in plant tissues, respiration fluxes and root free soil. We also assess plant N availability by comparing total leaf N pools and understorey leaf $\delta^{15}N$ values.

Site description

The experimental site is located within Siksik Creek catchment (68°44'54.5" N, 133°29'41.7" W), a small subsidiary of Trail Valley Creek, ~55 km NNE of Inuvik in Canada's NW Territories. The site is underlain by continuous permafrost with soils composed of 0.05–0.5 m organic-rich cryosols overlaying 1 m thick Quaternary Pleistocene till (Teare 1998). The topography of the catchment and surrounding area is characterized by gentle rolling hills, with a mean elevation of ~ 80 m above sea level. Siksik Creek is at the southern limit of Arctic bioclimatic subzone E (Walker *et al* 2005), just beyond the northern limit of the spruce treeline. Mean air temperatures were 16.7 °C for October 2013–April 2014, and 7.1 °C for May–September 2014 (Street *et al* 2016, Dean *et al* 2016).

Vegetation within Siksik Creek catchment is composed of heath tundra on hilltops, with ericaceous shrubs, sedges, prostrate *Salix* species and a well-developed lichen layer. Sedge and moss-dominated tundra is present in wetter areas. Patches of deciduous shrubs are a significant component of the landscape, consisting of green alder (*Alnus viridis* (Chaix) DC.), dwarf birch (*Betula glandulosa* Michx., B.) and *Salix* species. *A. viridis* and *B. glandulosa* are present in distinct patches on hillslopes or in riparian zones, while the taller *Salix* shrub species are confined to water tracks and riparian areas. We located our experimental plots in patches of alder- and birch-dominated vegetation on a gently-sloping south-west facing hillslope *ca.* 200 m from the Siksik Creek stream channel. The understorey vegetation was dominated by ericaceous *Rhododendron tomentosum* Harmaja and *Vaccinium vitis-idaea* L., with forbs (e.g. *Petasites frigidus* (L.) Fr.) and graminoids (including *Carex* spp.) also present.

Pulse-labelling

In order to trace the fate of photosynthetic carbon, we pulse-labelled replicate plots with CO_2 enriched in ^{13}C (> 99 atom%). We labelled four replicate 0.8 × 0.8 m plots in a patch of *A. viridis* and a nearby patch of *B. glandulosa* within *ca.* 100 m of each other. Individual plots were pulse-labelled over a two-hour period, and labelling was carried out over three consecutive days from 26–28 July 2013 following a block design to avoid bias from unavoidable variations in light and temperature conditions during this period. Further methodological details and environmental conditions during labelling (table S1) available at stacks.iop.org/ERL/13/084014/mmedia are given in supplementary material (appendix S2).

Tracing the fate of assimilated ^{13}C after labelling

We traced the fate of the assimilated ^{13}C label over time by sampling leaves ($n = 7$ time points), stems and roots of the dominant plant species ($n = 2$ time points). We quantified $\delta^{15}N$ on leaves and % N by mass on leaf and stem samples at a single time point (4 days after labelling). Eighteen days after labelling we removed soil cores (0.05 m diameter) to quantify the total ^{13}C remaining in total root biomass and in root-free SOM (fine roots were removed by hand from a small subsample of soil). We quantified the ^{13}C content (by manual gas sampling) of ecosystem respiration ($n = 3$ time points) and in belowground respiration ($n = 9$ time points), in subplots from which understorey aboveground biomass had been removed. Appendix S2 contains further details on isotopic sampling methods for plants, soils and respiration fluxes. Natural abundance ^{13}C isotope ratios were also quantified for all pools and fluxes from unlabelled *Betula* and *Alnus* plots ($n = 3$).

^{13}C in soil and biomass pools

The total mass of ^{13}C (mg ^{13}C m^{-2}) originating from the applied label ('pulse-derived') in soil and biomass pools is calculated as:

$$^{13}C_x = \frac{C_x}{1000} \times \frac{\varepsilon_x}{100} \quad (1)$$

where $^{13}C_x$ is the mass of pulse-derived ^{13}C (mg ^{13}C m^{-2}) in C pool x, C_x is the total mass of C contained in pool x (g C m^{-2}) and ε_x is the ^{13}C content of pool x in units of atom% excess above natural abundance. Total carbon pools sizes were quantified by destructive sampling (details in appendix S1). For leaf and stem pools, the total pulse-derived ^{13}C pool for the whole community was calculated as the sum of pulse-derived ^{13}C for leaf or stem pools of each species. Understorey species for which ^{13}C content was measured (*P. frigidus*, *R. tomentosum*, *V. vitis-idaea* plus graminoids) accounted for, on average, 94% of understorey leaf biomass—for species that were not sampled we assumed a ^{13}C atom% value equal to the average value for the other understorey species.

^{13}C in respiration fluxes

We used the Keeling plot method to quantify the ^{13}C isotope ratio of belowground and ecosystem respiration

(figure S3). This method assumes that the *y*-intercept of a linear regression between chamber headspace $\delta^{13}C$ and the inverse of CO_2 concentration provides an estimate of the isotopic composition of the respiration source (Pataki *et al* 2003). The pulse-derived ^{13}C respiration flux is then calculated as:

$$^{13}C_R = R \times \frac{\varepsilon_R}{100} \quad (2)$$

where $^{13}C_R$ is the respiratory ^{13}C flux (mg $^{13}C\,m^{-2}\,min^{-1}$), R is the total respiratory flux (mg $C\,m^{-2}\,min^{-1}$) and ε_{resp} is the ^{13}C content of the respiration source expressed as atom% excess above natural abundance.

We calculated the ^{13}C 'return flux' in ecosystem and belowground respiration, based on the ^{13}C content of respired CO_2 and measured/modelled respiration flux rates (details on respiration flux modelling are given in the supplementary material appendix S4).

We then express the ^{13}C content of plant biomass, soil and respiration fluxes as a percentage of total ^{13}C assimilated over the labelling period ($^{13}C_{uptake}$; mg $^{13}C\,m^{-2}$), which we assume is equal to total $^{13}C_{leaf}$ immediately after labelling (at $t = 0$). In reality, a small amount of ^{13}C label will move out of the leaves over the labelling period and the gross uptake of ^{13}C will be slightly underestimated. With a continuous two hour labelling period, there will be approximately one hour's worth of losses from leaves (either through respiration or translocation) on average over the labelling period. Based on the fitted values for ^{13}C retention in leaves over time (supplementary material appendix S3) we estimate ^{13}C loss from leaves during the labelling period to be ~ 5% (figure S6). We quantify CUE over the study period using the total label recovered from plant and soil pools after 18 days, and BPE as the total label recovered in plant biomass. We aimed to capture the dynamics of metabolically active plant C—i.e. photosynthesised C which is used to support plant respiration or growth (Ostler *et al* 2016)—and previous labelling experiments suggest that respiratory return of ^{13}C becomes undetectable after approximately this period (Street *et al* 2013).

Statistical analysis

All analyses were carried out in R version 3.3.1 (R Core Team 2016).We use linear mixed effects models to compare root and SOM $\delta^{13}C$ values. We use paired t-tests to assess differences in the total recovery of ^{13}C in respiration fluxes, soil and biomass pools, and ANOVA to compare understorey leaf N concentrations and $\delta^{15}N$ values.

Results

Carbon and nitrogen pools

Total aboveground biomass varied between 244–598 g C m^{-2} in the *Alnus* plots and 256–355 g C m^{-2} in the *Betula* plots. *A. viridis* stems contributed the largest single aboveground C pool, containing approximately double the amount of C found in *B. glandulosa* stems, but aboveground C in the leaves and stems of understorey species was similar between vegetation types (figure 1(*a*) and (*b*)). The root C pool in surface soils (0–0.15 m depth) was also similar between the vegetation types (*Alnus* 480 ± 231 g m^{-2}, *Betula* 433 ± 203 g m^{-2}), and there were no clear differences in root distributions with depth (figure 1(*c*)). Total SOM-C within the organic horizon was 3640 ± 1400 g C m^{-2} for *Alnus* and 3080 ± 4091 g C m^{-2} for *Betula* (figure 1(*d*)).

Total leaf N pools were similar between vegetation types with 2.8 ± 1.1 g N m^{-2} ground in *Alnus* and 2.9 ± 0.77 g N m^{-2} ground in *Betula.* ^{15}N isotope ratios differed between the dominant shrub species, with leaf $\delta^{15}N$ of −1.6 ± 0.27 ‰ for *A. viridis* and −8.9 ± 1.4 ‰ for *B. glandulosa* but there were no significant differences in understorey leaf N concentrations (ANOVA, F = 2.7, d.f. = 1, $p = 0.12$) or leaf $\delta^{15}N$ values (ANOVA, F = 0.27, d.f. = 1, $p = 0.62$) (figure 2). Stem N concentrations showed a similar pattern, with no clear differences except that *A. viridis* stem N concentrations (0.83 ± 0.1% dry wt.) were > 2 x stem N concentrations in *B. glandulosa* (0.41 ± 0.1% dry wt.) (figure S2).

^{13}C dynamics in leaves and stems

The total amount of ^{13}C label assimilated into leaf tissue across all plots was 40–141 mg $^{13}C\,m^{-2}$ (figure S4). Initial enrichment was followed by a consistent decline in leaf ^{13}C ratios over time for all species (figure S5). At the canopy-scale there was an initial rapid decrease in the fraction of assimilated ^{13}C retained within the leaves, then after 3–4 days leaf ^{13}C contents declined more gradually. ^{13}C enrichment was lower in stems than in leaf material (figure S7). *A. viridis* stems tended to have higher levels of enrichment than *B. glandulosa* stems, and in three of the four plots *A. viridis* ^{13}C content increased slightly between $t = 4$ and $t = 18$–19 (we identified one data point as an outlier, see figure S7); for *B. glandulosa* stem ^{13}C isotope ratios were similar between the two time-points (figure S7).

^{13}C enrichment in roots and soil

The $\delta^{13}C$ isotope values of bulk fine root material from *Alnus* plots were enriched by *ca.* 1.7 ‰ compared to natural abundance, though this was not statistically significant (figure S8(*a*), table S2). The $\delta^{13}C$ isotope values of fine roots from the *Betula* plots however increased by ~2.7 ‰, significant at $\alpha = 0.1$ (figure S8(*b*), table S2). We could detect no incorporation of ^{13}C in root-free SOM in the *Alnus* plots, with the overall effect of the labelling on SOM $\delta^{13}C$ being < 0.2 ‰ (figure S8(*c*)). In contrast, the $\delta^{13}C$ of SOM in the labelled *Betula* plots consistently increased by *ca.* 1.0 ‰ (table S2, figure S8(*d*)). We found only two *Alnus* root nodules in labelled soil cores, but levels of ^{13}C enrichment in these

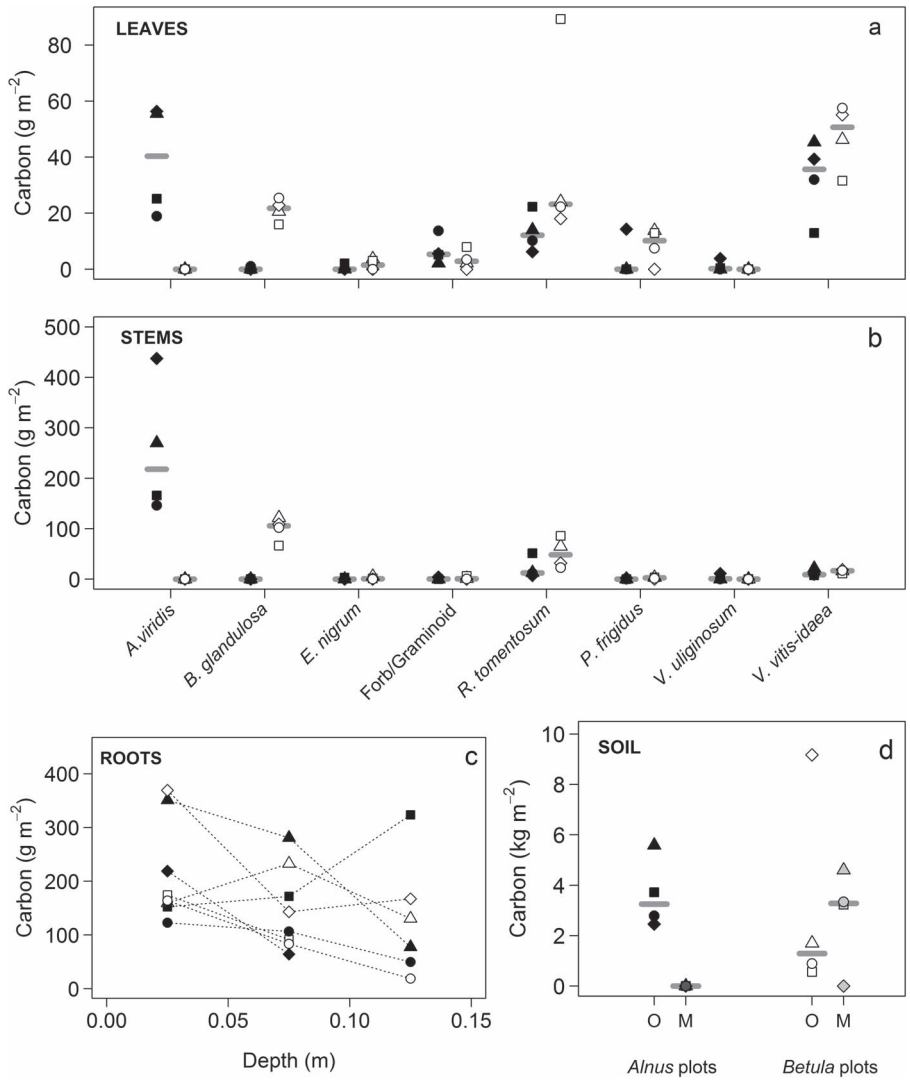

Figure 1. Above- and belowground C stocks for *Alnus* (filled symbols) and *Betula* (open symbols) vegetation plots: (*a*) leaf C stocks by species; (*b*) stem C stocks by species; (*c*) total root C stocks with soil depth and (*d*) organic (O) and mineral (M) carbon stocks in top 0.15 m of soil. Different shaped symbols indicate individual data points for four experimental replicates; the solid grey horizontal line indicates the median value. Dotted lines in panel (*c*) are to aid visualisation of the replicates rather than represent pattern with depth.

nodules were high at *ca.* 10 ‰ above natural abundance values (figure S8(*e*)).

^{13}C in respiratory fluxes

Belowground respiration rates (excluding understorey aboveground biomass) were 3.5 μmol CO_2 m^2 s^{-1} on average in the *Betula* plots and 3.0 μmol CO_2 m^{-2} s^{-1} in the *Alnus* plots; there were no clear difference in belowground respiration rates between vegetation types (figure S9). However, the percentage of assimilated ^{13}C recovered in belowground respiration was higher for the *Betula* plots (accounting for 26% of total label uptake) than for the *Alnus* plots (13% of total label uptake; $t = 2.89$, df = 3, $p = 0.06$; figure 3(*a*), figure S10). Measured ecosystem respiration rates varied between 1.2–4.8 μmol m^{-2} s^{-1} for *Alnus* and 0.6–8.5 μmol m^{-2} s^{-1} for *Betula*. ^{13}C ecosystem respiration fluxes however were consistently greater for *Alnus* than for *Betula* (figure S12). Over 18 days following labelling, the total ecosystem respiratory return of ^{13}C was significantly higher for the *Alnus* plots (39% of initial label uptake) than for the *Betula* plots (23% of initial label uptake; figure 3(*b*); paired ttest, $t = 3.35$, d.f. = 3, $p = 0.04$).

Partitioning of recent photosynthate in biomass after 18 days

Assimilated ^{13}C recovered from plant biomass pools (indicating BPE) over 18–19 days was 56 ± 14% for *Alnus* and 31 ± 2% for *Betula*, although this was not a statistically significant difference (two sample *t*-test, $t = 1.7$, d.f. = 3, $p = 0.22$). Both vegetation types retained a similar proportion of assimilated label in leaf and root pools (figure 4(*a*)). The two vegetation types differed significantly in the proportion of ^{13}C retained in stems, and in root-free SOM. In the *Betula* plots 28 ± 6% of the assimilated label was recovered from the root-free SOM component, accounting for a greater proportion of the total ^{13}C recovered than any other pool after

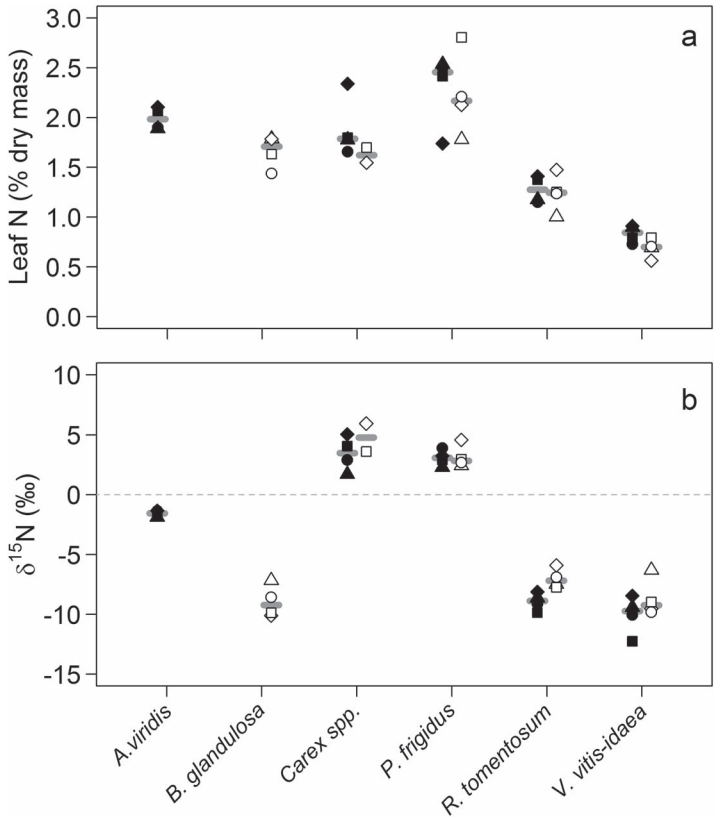

Figure 2. Leaf N characteristics for *Alnus* (black symbols) and *Betula* (open symbols) vegetation (*a*) leaf nitrogen concentration by species; and (*b*) leaf δ^{15}N by species for each vegetation type. Different shaped symbols indicate individual data points for four experimental replicates; the solid grey line indicates the median value.

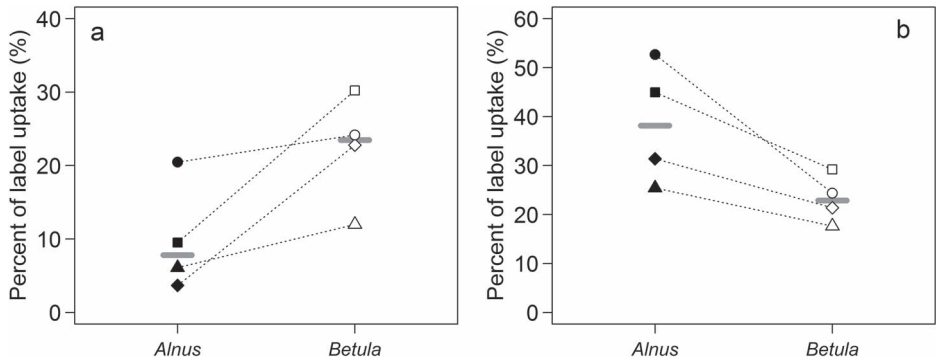

Figure 3. (*a*) Total ^{13}C respired belowground and (*b*) total ^{13}C respired by the ecosystem over 18 days following labelling as a percentage of the total uptake. Data points are individual experimental replicates—closed symbols are *Alnus* plots, open symbols are *Betula* plots. The dotted lines between symbols indicate paired data points (blocks) to add visualisation of the differences between vegetation types, as labelling conditions varied for each pair of plots; grey bars are median values.

18 days (figure 4(*b*)). In the *Alnus* plots there was no detectable excess ^{13}C in the root-free soil (figure 4(*a*)) and instead stem biomass accounted for the largest fraction of recovered ^{13}C (27 ± 5%). Total recovery of assimilated ^{13}C in all plant and soil pools, or the CUE over 18 days, did not differ between vegetation types, 56 ± 12% for *Alnus* and 59 ± 6% for *Betula* (two sample *t*-test, $t = 0.20$, d.f. = 3, $p = 0.85$). The unrecovered component of assimilated label (i.e. assimilated ^{13}C not detected in soil, biomass or respiration) was on average 8% for *Alnus* and 16% for *Betula* (figure 4(*b*)).

Discussion

Patterns of plant C allocation between ecosystem components will determine the impact on Arctic C

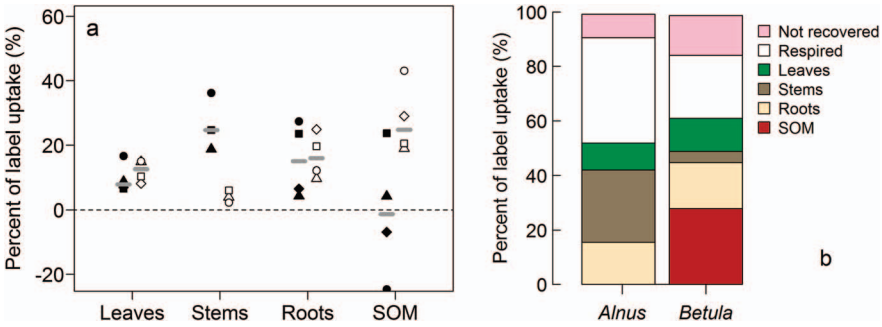

Figure 4. The fate of assimilated ^{13}C in biomass and soils after 18 days expressed as a percentage of the total ^{13}C assimilated (*a*) ^{13}C retention in plant and soil pools plotted as individual data points—closed symbols are *Alnus* plots, open symbols are *Betula* plots, with different shaped symbols corresponding to four experimental blocks; the grey line indicates the median value. (*b*) ^{13}C retention in plant and soil pools, and ^{13}C recovery in ecosystem respiration as an average of total ^{13}C uptake. SOM = root-free soil organic matter (which includes fungal hyphae).

balance if tundra vegetation becomes more productive. Our expectation was that the presence of an N-fixing shrub would lead to greater biomass production per unit photosynthesis (BPE) compared to an ECM-shrub dominated community. While our data do suggest that BPE in *Betula* vegetation may have been lower than in *Alnus*, (31% *vs.* 56%) we did not measure a statistically significant difference. As we expected, CUE over the study period did not differ between *Alnus* and *Betula* vegetation and was slightly greater than 50%, consistent with previous work (van Oijen *et al* 2010).

There were, however, clear differences in the fate of C once fixed as NPP. Around twice the amount of ^{13}C label (as a proportion of the total photosynthesised) was allocated aboveground in *Alnus*, mainly as a result of allocation to stem biomass (the amount of label in leaves after 18 days was similar between vegetation types). *A. viridis* stems comprised the single largest aboveground biomass pool and contained about double the total amount of C in *B. glandulosa* stems, so it is perhaps unsurprising to find a greater absolute sink for recent photosynthate in stems in *Alnus* vegetation. However, the allocation of photosynthate to stems was greater than would be expected on the basis of differences in stem biomass, being four to five times as high in *Alnus* compared to *Betula.* This is reflected in the higher isotopic enrichment in *A. viridis* stem tissue ($> 5 \times 10^{-3}$ atom% excess) compared to *B. glandulosa* ($< 5 \times 10^{-3}$ atom% excess, figure S7) and suggests that *Alnus* has a higher photosynthate requirement per unit stem mass. The N concentration of *A. viridis* stem tissue was approximately double that of *B. glandulosa*, and significantly higher than any of the other woody species in these communities, which also suggests higher metabolic demand (Reich *et al* 2008). Higher allocation of photosynthate to stem biomass in *Alnus* plots, therefore likely reflects more rapid growth in *A. viridis*, a greater allocation of photosynthate to stem storage pools (e.g. as non-structural carbohydrate), or a combination of both. High rates of allocation to rapidly respiring stem tissue also explains why total ^{13}C in ecosystem respiration fluxes was higher for *Alnus* than for *Betula*, even though ^{13}C in the belowground respiration flux was lower in the *Alnus* plots.

A further striking difference between shrub types in C allocation patterns was the substantial fraction of recent photosynthate recovered from root-free soil under *Betula.* The root-free soil pool we sampled includes fungal hyphae, microbial biomass and SOM, and incorporates many possible forms of non-plant biomass C. Whilst we did not measure enrichment in ECM hyphae directly, it is reasonable to assume that the extensive mycorrhizal networks which form under *Betula* (Deslippe and Simard 2011) facilitate the transfer of C from roots into the rhizosphere, and that ECM enrichment contributes to the ^{13}C signal we observed. The lack of detectable ^{13}C in *Alnus* soil suggests that in these communities the amount of recent photosynthate allocated to rhizosphere pools is very much smaller; so, while *Alnus* does associate with ECM (Horton *et al* 2013), in this context it seems likely that *Alnus* fungal symbionts do not receive the same C subsidy as the fungal community associated with *Betula.*

We did not recover all of the photosynthesized ^{13}C label from either vegetation type, probably because some label was transported outside of the plots. The logistical difficulties of working at a remote site restricted the size of the plots we could label, and if we had trenched around the plot margin we would have severely damaged the plants. It is likely then that at least some ^{13}C was transported outside of the plot (or deeper within the soil) via roots, hyphae, or diffusion of dissolved organic carbon or CO_2 (methane production in these mid-hill slope positions is low (Street *et al* 2016)) and the importance of these pathways may have differed between plots. The 'unrecovered' component was greater in *Betula*, which might be expected given that the ^{13}C was distributed more widely through the bulk soil, probably via hyphal networks; *B. nana* for example has been shown to transfer around 10% of photosynthate between individual plants via hyphae (Deslippe and Simard 2011).

Isotopic labelling experiments such as this involve multiple potential sources of error and bias as a result of the many different kinds of measurement required to quantify the fate of ^{13}C across multiple fluxes and pools. We mention here some the most important limitations that should be considered. Firstly, our estimate of total gross ^{13}C uptake at $t = 0$ is likely an underestimate, because leaves will have lost carbon through respiration during the labelling period. We estimate this bias to be small (less than 5%) but if gross ^{13}C uptake is underestimated by 5%, our estimates of CUE/BPE will be overestimated by ~ 3 percentage points (i.e. for *Betula* CUE would be 53%, rather than 56%). A further potential bias in our results arises because of the impact of vegetation removal within respiration collars on our estimates of belowground ^{13}C respiration fluxes. The removal of understorey vegetation likely reduces the ^{13}C return flux that would be measured were the vegetation intact. However, because understorey vegetation composition is similar between vegetation types, the impact of this is likely to be similar for both vegetation types. Vegetation removal is very unlikely to have significantly influenced measurements of ecosystem ^{13}C respiration fluxes, because the area affected (that inside the respiration collars) was < 2.5% of the total area of the labelled plot and the dominant shrub vegetation remained completely intact. The quantification of ecosystem ^{13}C fluxes was challenging, because we were only able to measure fluxes at three time points, and we rely on the model of Shaver *et al* (2013) to quantify the total return flux. This uncertainty does not impact our estimates of CUE/BPE however because these were based on tissue and soil data.

It was beyond the scope of this study to quantify N_2 fixation rates, but several lines of evidence suggest that the *A. viridis* plants at this site derive a substantial component of their N budget from fixation. An observed leaf $\delta^{15}N$ value of −1.6‰ is typical of N_2 fixing species which derive N only from fixation (Boddey *et al* 2000), and is much closer to zero (i.e. to atmospheric values) than any other species in these communities. The presence of root nodules and high ^{13}C enrichment in those nodules after labelling also indicate that photosynthate was being allocated to support N_2 fixation. We only recovered two nodules in our soil cores, so our estimates are uncertain, but on the basis of the mass of the nodules collected (average mass of 4 mg dry weight), a rough estimate of total nodule biomass per plot in the top 0.15 m of soil would be ~2.5 mg m^{-2} (this is lower than in boreal regions where nodule biomass has been recorded up to 44 g m^{-2} (Mitchell and Ruess 2009a)). The allocation of C to root nodules in our plots would then account for roughly 0.3% of recent photosynthesis.

We did not find clear evidence that the presence of N-fixing *A. viridis* plants had an impact on N availability at the community level; understorey species composition and abundance were very similar to the *Betula* understorey, and there were no differences in understorey leaf N concentrations or $\delta^{15}N$ values between vegetation types. The total amount of leaf N per unit ground area was also very similar between vegetation types. This suggests that the predominant mode of N acquisition (i.e. fixation vs. root/ectomycorrhizal uptake), rather than N availability *per se*, drives the differences in C allocation between these shrub types.

The continuing deepening of the Active layer and associated increase in nutrient availability (Schuur *et al* 2015) is projected to increase the expansion of deciduous shrubs in the circumpolar Arctic region. Recent modelling runs indicate a significant increase in the proportion of primary productivity associated with deciduous shrub species in tundra ecosystems over the 21st century (Mekonnen *et al* 2018). Our findings show that estimates of NPP associated with 'shrub' expansion are simplistic, and that it is critical to incorporate cascading impacts of productivity changes on belowground dynamics of C and N for specific shrub genera to predict ecosystem responses and feedbacks with the climate system.

In conclusion, we did not find evidence for a difference in CUE between the two vegetation types—thus, as shrubs encroach on tundra ecosystems, we would expect similar total inputs of fixed C to the ecosystem for every unit of additional GPP, regardless of shrub species. However, we did find clear differences in the fate of C photosynthesised as NPP. We show that not only does belowground allocation differ markedly between these shrub species, but also the distribution of that C throughout the soil profile. In *Alnus* dominated vegetation, recent photosynthate allocated belowground largely remains incorporated in plant root tissue, whereas in *Betula* it is distributed widely throughout the bulk soil. The amount and distribution of labile plant C inputs belowground therefore imply that the potential for priming of SOM (Hartley *et al* 2012) under *Betula* is much greater. Organic soils tended to be thinner in our *Betula* plots, suggesting faster turnover of SOM pools, and this is consistent with previous studies (Parker *et al* 2015, Hartley *et al* 2012). Our study implies that as Arctic vegetation changes, these common shrub species will differ significantly in their influence on ecosystem C dynamics, even if increases in aboveground productivity (=greening) are similar.

Acknowledgments

This work was funded by NERC grant NE/K000284/1 (P A Wookey) as part of the NERC Arctic Research Programme. We would like to thank the staff at the Aurora Research Institute, as well as Prof Philip Marsh and Prof Oliver Sonnentag, for providing logistical support and advice. We also thank Nicolas Pelletier and Ian Washbourne for their assistance with fieldwork. L S, J A S and P W conceived and designed the study, L S, J A S, P W, R B, K D and C K carried out fieldwork,

laboratory analysis and data analysis. All authors contributed to writing the manuscript.

ORCID iDs

Lorna E Street https://orcid.org/0000-0001-9570-7479
Jens-Arne Subke https://orcid.org/0000-0001-9244-639X
Robert Baxter https://orcid.org/0000-0002-7504-6797
Christian Knoblauch https://orcid.org/0000-0002-7147-1008
P A Wookey https://orcid.org/0000-0001-5957-6424

References

Abbott B W *et al* 2016 Biomass offsets little or none of permafrost carbon release from soils, streams, and wildfire: an expert assessment *Environ. Res. Lett.* **11** 034014

Boddey R M, Peoples M B, Palmer B and Dart P J 2000 Use of the ^{15}N natural abundance technique to quantify biological nitrogen fixation by woody perennials *Nutr. Cycl. Agroecosyst.* **57** 235–70

Bradford M A and Crowther T W 2013 Carbon use efficiency and storage in terrestrial ecosystems *New Phytol.* **199** 7–9

Campioli M *et al* 2015 Biomass production efficiency controlled by management in temperate and boreal ecosystems *Nat. Geosci.* **8** 843–6

Dean J F, Billett M F, Baxter R, Dinsmore K J, Lessels J S, Street L E, Subke J-A, Tetzlaff D, Washbourne I and Wookey P A 2016 Biogeochemistry of 'pristine' freshwater stream and lake systems in the western Canadian Arctic *Biogeochemistry* **130** 191–213

Deslippe J R and Simard S W 2011 Below-ground carbon transfer among *Betula* nana may increase with warming in Arctic tundra *New Phytol.* **192** 689–98

Forbes B C, Fauria M M and Zetterberg P 2010 Russian Arctic warming and 'greening' are closely tracked by tundra shrub willows *Glob. Change Biol.* **16** 1542–54

Fraser R H, Lantz T C, Olthof I, Kokelj S V and Sims R A 2014 Warming-induced shrub expansion and lichen decline in the western Canadian Arctic *Ecosystems* **17** 1151–68

Faubert P, Tiiva P, Michelsen A, Rinnan Å, Ro-Poulsen H and Rinnan R 2012 The shift in plant species composition in a subarctic mountain birch forest floor due to climate change would modify the biogenic volatile organic compound emission profile *Plant Soil* **352** 199–215

Hartley I P, Garnett M, Sommerkorn M, Hopkins D W, Fletcher B J, Sloan V L, Phoenix G K and Wookey P A 2012 A potential loss of carbon associated with greater plant growth in the European Arctic *Nat. Clim. Change* **2** 875–9

Hobbie J E, Kwiatkowski B L, Rastetter E B, Walker D A and McKane R B 1998 Carbon cycling in the Kuparuk basin: plant production, carbon storage, and sensitivity to future changes *J. Geophys. Res.* **103** 29065–73

Horton T R, Hayward J, Tourtellot S G and Taylor D L 2013 Commentary uncommon ectomycorrhizal networks : richness and distribution of *Alnus*-associating ectomycorrhizal fungal communities *New Phytol.* **198** 2012–4

Jia G J, Epstein H E and Walker D A 2009 Vegetation greening in the Canadian Arctic related to decadal warming *J. Environ. Monit.* **11** 2231

Koven C D, Ringeval B, Friedlingstein P, Ciais P, Cadule P, Khvorostyanov D, Krinner G and Tarnocai C 2011 Permafrost carbon-climate feedbacks accelerate global warming *Proc. Natl Acad. Sci. USA* **108** 14769–74

Kuzyakov Y, Friedel J K and Stahr K 2000 Review of mechanisms and quantification of priming effects *Soil Biol. Biochem.* **32** 1485–98

Lantz T C, Marsh P and Kokelj S V 2013 Recent shrub proliferation in the Mackenzie Delta uplands and microclimatic implications *Ecosystems* **16** 47–59

Mekonnen Z A, Riley W J and Grant R F 2018 Accelerated nutrient cycling and increased light competition will lead to 21st century shrub expansion in North American Arctic tundra *J. Geophys. Res. Biogeosci.* **123** 1683–701

Mitchell J S and Ruess R W 2009a N_2 fixing alder (*Alnus viridis* spp. *fruticosa*) effects on soil properties across a secondary successional chronosequence in interior Alaska *Biogeochemistry* **95** 215–29

Mitchell J S and Ruess R W 2009 b Seasonal patterns of climate controls over nitrogen fixation by *Alnus viridis subsp fruticosa* in a secondary successional chronosequence in interior Alaska *Ecoscience* **16** 341–51

Myers-Smith I H *et al* 2011 Shrub expansion in tundra ecosystems: dynamics, impacts and research priorities *Environ. Res. Lett.* **6** 45509

van Oijen M, Schapendonk A and Höglind M 2010 On the relative magnitudes of photosynthesis, respiration, growth and carbon storage in vegetation *Ann. Bot.* **105** 793–7

Ostler U, Schleip I, Lattanzi F A and Schnyder H 2016 Carbon dynamics in aboveground biomass of co-dominant plant species in a temperate grassland ecosystem: same or different? *New Phyt.* **210** 471–84

Pataki D E, Ehleringer J R, Flanagan L B, Yakir D, Bowling D R, Still C J, Buchmann N, Kaplan J O and Berry J A 2003 The application and interpretation of keeling plots in terrestrial carbon cycle research *Glob. Biogeochem. Cycles* **17** 1022

Parker T C, Subke J A and Wookey P A 2015 Rapid carbon turnover beneath shrub and tree vegetation is associated with low soil carbon stocks at a subarctic treeline *Glob. Chang. Biol.* **21** 2070–81

R Core Team 2016 R: A language and environment for statistical computing (Vienna: R Foundation for Statistical Computing)

Reich P B, Tjoelker M G, Pregitzer K S, Wright I J, Oleksyn J and MaChado J L 2008 Scaling of respiration to nitrogen in leaves, stems and roots of higher land plants *Ecol. Lett.* **11** 793–801

Roxburgh S H, Berry S L, Buckley T N, Barnes B and Roderick M L 2005 What is NPP? Inconsistent accounting of respiratory fluxes in the definition of net primary production *Funct. Ecol.* **19** 378–82

Schaefer K, Zhang T, Bruhwiler L and Barrett A P 2011 Amount and timing of permafrost carbon release in response to climate warming *Tellus, Ser. B Chem. Phys. Meteorol.* **63** 165–80

Schuur E A G, McGuire A D, Grosse G, Harden J W, Hayes D J, Hugelius G, Koven C D and Kuhry P 2015 Climate change and the permafrost carbon feedback *Nature* **520** 171–9

Shaver G R, Rastetter E B, Salmon V, Street L E, van de Weg M J, Rocha A, van Wijk M T and Williams M 2013 Pan-Arctic modelling of net ecosystem exchange of CO_2 *Philos. Trans. R. Soc.* B **368** 20120485

Street L E, Dean J F, Billett M F, Baxter R, Dinsmore K J, Lessels J S, Subke J-A, Tetzlaff D and Wookey P A 2016 Redox dynamics in the active layer of an Arctic headwater catchment; examining the potential for transfer of dissolved methane from soils to stream water *J. Geophys. Res. Biogeosci.* **121** 2776–92

Street L E, Subke J A, Sommerkorn M, Sloan V, Ducrotoy H, Phoenix G K and Williams M 2013 The role of mosses in carbon uptake and partitioning in arctic vegetation *New Phytol.* **199** 163–75

Sturm M, Racine C and Tape K 2001 Climate change. Increasing shrub abundance in the Arctic *Nature* **411** 546–7

Teare C 1998 Spatial and temporal patterns of chemical solute signals in sixteen small tundra streams of the Trail Valley

Creek watershed in the Western Canadian Arctic *Masters Thesis* (Vancouver: Simon Fraser University)

Vicca S *et al* 2012 Fertile forests produce biomass more efficiently *Ecol. Lett.* **15** 520–6

Walker D A *et al* 2005 The circumpolar Arctic vegetation map *J. Veg. Sci.* **16** 267–82

Walker T N, Garnett M H, Ward S E, Oakley S, Bardgett R D and Ostle N J 2016 Vascular plants promote ancient peatland carbon loss with climate warming *Glob. Change Biol.* **22** 1880–9

Wilmking M, Harden J and Tape K 2006 Effect of tree line advance on carbon storage in NW Alaska *J. Geophys. Res. Biogeosci.* **111** 1–10

Xia J *et al* 2017 Terrestrial ecosystem model performance in simulating productivity and its vulnerability to climate change in the northern permafrost region *J. Geophys. Res. Biogeosci.* **122** 430–46